Repurposing CD19-directed immunotherapies for pediatric t(8;21) acute myeloid leukemia

Farnaz Barneh[1#], Joost B. Koedijk[1,2#], Noa E. Wijnen[1,3#], Tom Meulendijks[1], Minoo Ashtiani[1], Ester Dunnebach[1,4], Noël Dautzenberg[1], Annelisa M. Cornel[1,4], Anja Krippner-Heidenreich[1], Kim Klein[1,5], C. Michel Zwaan[1,2], Jürgen Kuball[4], Stefan Nierkens[1,4], Jacqueline Cloos[6], Gertjan J.L. Kaspers[1,3]*, Olaf Heidenreich[1,7,8]*

[#]Shared first-authorship; *Shared senior-authorship

1. Princess Máxima Center for Pediatric Oncology, Utrecht, The Netherlands
2. Erasmus MC-Sophia Children's Hospital, Department of Pediatric Oncology, Rotterdam, The Netherlands
3. Emma Children's Hospital, Amsterdam UMC, Vrije Universiteit, Department of Pediatric Oncology, Amsterdam, The Netherlands
4. Center for Translational Immunology, University Medical Center Utrecht, Utrecht University, Utrecht, The Netherlands
5. Wilhelmina Children's Hospital/University Medical Center, Utrecht, The Netherlands
6. Department of Hematology, Amsterdam UMC, Vrije Universiteit Amsterdam, Cancer Center Amsterdam, The Netherlands
7. Wolfson Childhood Cancer Research Centre, Translational and Clinical Research Institute, Newcastle University, Newcastle upon Tyne, United Kingdom
8. University Medical Center Utrecht, Utrecht University, Utrecht, The Netherlands

Corresponding authors:

G.J.L. Kaspers, Princess Máxima Center for Pediatric Oncology, Heidelberglaan 25, 3584 CS Utrecht, The Netherlands. E-mail: g.j.l.kaspers@prinsesmaximacentrum.nl; Tel: +31889727272

O. Heidenreich, Princess Máxima Center for Pediatric Oncology, Heidelberglaan 25, 3584 CS Utrecht, The Netherlands.E-mail: O.T.Heidenreich@prinsesmaximacentrum.nl; Tel: +31683069960

Short title: Targeting CD19 in t(8;21) AML

Disclosure of interest: The authors declare no conflicts of interest.

Funding: This work has been funded by a KIKA (329) program grant to O.H.

Word count: 4307 (main text), 232 (abstract). **Figures:** 6 main figures, 4 supplementary figures. **Tables:** 1 main table, 3 supplementary tables. **Supplementary Methods:** 1 file.

Abstract

In contrast to patients with B cell precursor acute lymphoblastic leukemia (BCP-ALL), patients with acute myeloid leukemia (AML) have not yet benefited from recent advances in targeted immunotherapy. Repurposing immunotherapies that have been successfully used to target other hematological malignancies could, in case of a shared target antigen, represent a promising opportunity to expand the immunotherapeutic options for AML. Here, we evaluated the expression of CD19 in a large pediatric AML cohort, assessed the *ex vivo* AML killing efficacy of CD19-directed immunotherapies, and characterized the bone marrow immune microenvironment in pediatric AML, BCP-ALL, and non-leukemic controls. Out of 167 newly diagnosed *de novo* pediatric AML patients, 18 patients (11%) had $CD19^+$ AML, with 61% carrying the translocation t(8;21)(q22;q22). Among $CD19^+$ samples, we observed a continuum of CD19 expression levels on AML cells. In individuals exhibiting unimodal and high CD19 expression, the antigen was consistently present on nearly all $CD34^+CD38^-$ and $CD34^+CD38^+$ subpopulations. In *ex vivo* AML-T cell co-cultures, blinatumomab demonstrated substantial AML killing, with an efficacy similar to BCP-ALL. In addition, CAR T cells could effectively eliminate $CD19^+$ AML cells *ex vivo*. Furthermore, our immunogenomic assessment of the bone marrow immune microenvironment of newly diagnosed pediatric t(8;21) AML revealed that T- and NK cells had a less exhausted and senescent phenotype in comparison to pediatric BCP-ALL. Altogether, our study underscores the promise of CD19-directed immunotherapies for the treatment of pediatric $CD19^+$ AML.

Keywords: children, tumor immune microenvironment, blinatumomab, CAR T cells, tumor antigens

Introduction

Although the survival of children with acute myeloid leukemia (AML) has improved considerably over the past decades, 25-35% of patients face relapse, which still has an unfavorable prognosis.[1-3] In addition, current high-dose chemotherapy and allogeneic stem cell transplantation (allo-SCT) regimens lead to significant side and late effects, together illustrating the need for more effective and less toxic therapeutic options.[3] Nontransplant, targeted immunotherapies such as bispecific antibodies and CAR T cells are of interest given their successes in both solid and hematological malignancies.[4-6] However, the development of targeted immunotherapy for AML has been challenging, mainly due to the paucity of tumor-specific antigens, on-target off-leukemia hematotoxicity when targeting myeloid-lineage antigens, and the immunosuppressive tumor microenvironment.[7, 8] Accordingly, with the exception of the CD33-directed antibody-drug-conjugate gemtuzumab ozogamicin, no targeted immunotherapeutic agents have been approved for adults or children with AML.[9, 10] Hence, repurposing immunotherapies that have been successfully used to target other hematological malignancies could, in case of a shared target antigen, represent a promising opportunity to expand the immunotherapeutic options for AML.

CD19 is a B cell marker which is highly expressed on B cell precursor acute lymphoblastic leukemia (BCP-ALL) cells. For children and adults with BCP-ALL, the CD19-directed bispecific T cell-engager blinatumomab (CD3 x CD19) and CD19-directed chimeric antigen receptor (CAR) T cells (tisagenlecleucel) demonstrated promising results in both pediatric and adult BCP-ALL, which ultimately led to their clinical approval.[6, 11-15] In AML, expression of CD19 is characteristic for t(8;21)(q22;q22), the most common translocation in children with this disease.[16] Interestingly, two case studies have reported complete molecular responses in two adults with relapsed $CD19^{+}$ t(8;21) AML following treatment with either blinatumomab or CD19-directed CAR T cells.[17, 18] Furthermore, two clinical trials are currently investigating the efficacy of CD19-directed CAR T

cells in relapsed and refractory (R/R) adult AML (NCT04257175 and NCT03896854). In several pediatric hematological malignancies including AML, another clinical trial is testing a combination of T cell-directed immunotherapies including blinatumomab in R/R CD19$^+$ patients after allo-SCT (NCT02790515). Apart from these case studies and ongoing trials, CD19-directed immunotherapies have not yet been studied in pediatric or adult AML and therefore, its efficacy in AML remains unknown.

Here, we examined the expression of CD19 on AML cells in a large cohort of children with newly diagnosed *de novo* AML, evaluated the *ex vivo* efficacy of CD19-directed immunotherapies, and characterized the bone marrow (BM) immune microenvironment in pediatric AML, BCP-ALL, and non-leukemic controls. Our work reveals pediatric t(8;21) AML as a subgroup with a high percentage of CD19$^+$ patients, and CD19$^+$ t(8;21) AML to be sensitive to blinatumomab- and CAR T cell-mediated cytotoxicity. Furthermore, our immunogenomic analyses of the BM immune microenvironment show that T- and NK cells in pediatric t(8;21) AML have a less exhausted and senescent phenotype in comparison to pediatric BCP-ALL. Altogether, our study demonstrates the potential of CD19-directed immunotherapies for the treatment of pediatric CD19$^+$ t(8;21) AML.

Materials and Methods

Ethical regulations

This study complied with all relevant ethical regulations and was approved by the Institutional Review Board of the Princess Máxima Center (PMCLAB2021.207, PMCLAB2021.258, and PMCLAB2022.334).

Clinical and flow cytometry data

A retrospective medical records analysis identified pediatric patients with newly diagnosed *de novo* AML treated in Dutch hospitals between January 2012 and October 2022 (details on

treatment regimen and response definitions are provided in Supplementary Methods). Reports of flow cytometry data collected in the diagnostic and, if applicable, relapse setting were retrieved to screen patients for CD19 positivity according to the guideline for assessment of marker positivity by the Dutch Foundation for Quality Assessment in Medical Laboratories (SKML; Supplementary Methods).[19]

CD19 expression analysis

The flow cytometry standard files, which were accessible for seven t(8;21) AML patients in the total study cohort, were utilized to examine the CD19 expression on myeloid blasts. Flow cytometry results were analyzed using FlowJo™ (v10.10 Software; BD Life Sciences) or Kaluza Analysis software (v2.2.1.20183; Beckman Coulter). The gating strategy for defining AML blasts is shown in **Figure 3A**. The coverage of CD19 expression among AML subpopulations was further determined by analyzing BM mononuclear cells (MCs) from two t(8;21) AML patients and one t(8;21) AML patient-derived xenograft (PDX) sample (RL048)[20] by flow cytometry (Cytoflex LX, Beckman Coulter; antibodies provided in Supplementary Methods).

***Ex vivo* T cell killing assays**

For allogeneic killing assays, healthy donor $CD3^+$ T cells isolated from healthy donors were first expanded using a previously published rapid expansion protocol.[21] Subsequently, T cells were co-cultured with $CD19^+$ primary t(8;21) AML BMMCs, RL048 PDX cells, or primary BCP-ALL BMMCs, at various effector-to-target (E:T) ratios (Supplementary Methods). Next, blinatumomab (1 nM; Blincyto®, Amgen) was added to the co-cultures for 48 hours, and co-cultures in the absence of blinatumomab were used to determine the extent of background killing. In autologous killing assays with primary BMMCs, blinatumomab (1 nM) was added directly to unsorted samples (1×10^5 BMMCs per well on a 96-well plate) to activate T cells present in the sample. The viability

of blinatumomab-treated samples was normalized to conditions without blinatumomab. Details on the T cell activation and Interferon-γ secretion procedures are provided in Supplementary Methods.

Bulk RNA-sequencing

Bulk RNA-sequencing (RNA-seq) and data analysis was performed according to the institute's standard pipelines.[22, 23] Details on the comparison of gene expression profiles between $CD19^{+}$- and $CD19^{-}$ t(8;21) AML are provided in Supplementary Methods. To characterize the BM immune microenvironment of patients with $CD19^{+}$- and $CD19^{-}$ t(8;21) AML (n=10), AML with other genotypes (n=30; cytogenetic data and other clinical parameters are shown in **Supplementary Table 1**), BCP-ALL (n=209; cytogenetic data and other clinical parameters are depicted in **Supplementary Table 2**), and non-leukemic controls (n=4)[26], we applied the immune deconvolution platform CIBERSORTx (cibersortx.stanford.edu; LM22 reference signature) to estimate the abundance of lymphoid populations and the TIDE algorithm to infer the abundance of several myeloid and stromal cell types (tide.dfci.harvard.edu; rationale for selected cell populations and details of other immune-based scores are provided in Supplementary Methods).[27-30]

Statistical analyses

All data were analyzed using the SPSS software (v26.0.0.1; IBM, USA) and GraphPad Prism (v8.0.2; GraphPad Software, USA). Two-sided *P* values of < 0.05 were considered statistically significant. Details of statistical methods and tests are provided in Supplementary Methods.

Results

CD19 expression is enriched in pediatric t(8;21) AML

To investigate CD19 as a potential target antigen in pediatric AML, we examined 167 *de novo* pediatric AML patients for CD19 positivity at diagnosis and, when applicable, at relapse. Using records of diagnostic flow cytometry data, we identified 18 newly diagnosed patients (11%) with $CD19^+$ AML cells (n=8 with CD19 median fluorescence intensity (MFI) difference (Δ) between leukemic blasts and healthy population of >10-fold, n=10 with ΔMFI of 3 to 10-fold; **Figure 1A)**. We next explored whether CD19 expression was associated with specific cytogenetic alterations. In line with data in adult AML, we found that 61% (n=11) of $CD19^+$ patients carried the translocation t(8;21)(q22;q22) (n=3: CD19 ΔMFI >10-fold, n=8: 3 to 10-fold; **Figure 1B**).[33, 34] Other cytogenetic alterations of $CD19^+$ pediatric AML patients included t(9;11)(p22;q23) (n=2), t(16;21)(q24;q22) (n=2), t(1;11)(q21;q23) (n=1), inv(16)(p13;q22) (n=1), and in one case cytogenetic information was not available (**Figure 1B**; additional clinical characteristics are listed in **Table 1**). In the entire cohort, 21 out of 167 patients had the (8;21) translocation, indicating that 52% of patients with this translocation were $CD19^+$ (**Figure 1C)**.

Regarding patient outcomes of $CD19^+$ AML patients, all (n=18) achieved complete remission (CR) by the end of the second induction course (100%), and there were no early deaths. Among the patients with $CD19^+$ AML at diagnosis, five experienced disease relapse (**Figure 1A**). In two of these cases, AML cells retained CD19 positivity, and both patients are currently alive. Conversely, in three cases, AML cells lost their CD19 expression at relapse. One of these patients deceased, which was the only death among patients with $CD19^+$ AML at diagnosis. Intriguingly, three patients with $CD19^-$ AML at diagnosis gained CD19 positivity at relapse (out of 33 relapses in the $CD19^-$ AML group), with a fatal outcome in one of these patients.

Next, we investigated whether CD19 expression on AML cells was associated with event-free survival (EFS) and overall survival (OS). To account for the confounding effect of cytogenetic alterations, we compared EFS and OS among all t(8;21) patients (n=21). In this exploratory analysis, the 5-year EFS and 5-year OS for the $CD19^+$ (n=11) and $CD19^-$ (n=10) groups were 65% (SE 17) and 74% (SE 16), and 100% and 89% (SE 11), respectively, showing no substantial difference, although the cohort size was limited (**Figure S1A-B**). Taken together, our data reveal an enrichment of CD19 positivity in pediatric t(8;21) AML at diagnosis, and gain of CD19 expression in relapsed cases with $CD19^-$ disease at initial diagnosis.

$CD19^+$ t(8;21) AML exhibits reduced metabolic activity and cell division

We next sought to further characterize differences between $CD19^+$ and $CD19^-$ t(8;21) AML. Specifically, given the typical expression of B cell-related genes such as *CD19* and *PAX5*, a B lymphoid transcription factor responsible for *CD19* upregulation, in t(8;21) AML, we aimed to investigate whether gene expression programs seen in (pre-)B cells were present in $CD19^+$ t(8;21) AML. To investigate this, we retrieved BM bulk RNA-sequencing data of patients with $CD19^+$- and $CD19^-$ t(8;21) AML and a blast percentage of at least 75% (n=6 vs. n=3, respectively). As anticipated, differential gene expression analysis revealed significant upregulation of the B cell-related genes *CD19* and *POU2AF1* in $CD19^+$ t(8;21) AML, as well as a trend towards higher expression of *PAX5 (***Figure 2A-B** and **Supplementary Table 3**).[35] Furthermore, GSEA showed that $CD19^+$ t(8;21) AML demonstrated a decrease in various metabolic processes including oxidative phosphorylation and fatty acid metabolism in comparison to $CD19^-$ t(8;21) AML, suggestive of lower metabolic activity in $CD19^+$ t(8;21) AML (**Figure 2C** and **Figure S2**). These data are consistent with previous work showing that *PAX5* enforces a state of chronic energy deprivation in pre-B cells.[36] In addition, cell cycle-related pathways were depleted in $CD19^+$- compared to $CD19^-$ t(8;21) AML, together suggesting a less proliferative state in $CD19^+$ t(8;21)

AML (**Figure 2C** and **Figure S2**). Given that such cells show in general less susceptibility to conventional chemotherapy, these data suggest that alternative therapies such as immunotherapies could be a suitable treatment option for $CD19^+$ AML.[37]

CD19 is expressed among different t(8;21) AML subpopulations

To evaluate the suitability of CD19 as an immunotherapeutic target, we next aimed to characterize the CD19 expression levels in $CD19^+$ t(8;21) AML. To do so, we re-analyzed diagnostic flow cytometry data available for six $CD19^+$ t(8;21) AML patients (patient #01-06) and one $CD19^-$ t(8;21) AML patient (patient #07; control), which allowed for investigating the expression of CD19 on $CD45^{dim}SSC\text{-}A^{low}CD34^+$ cells, and compared this to BMMC-derived $CD19^+$ B- and $CD19^-$ T cells (from patient #01) as a representative positive and negative control, respectively. The cell surface expression of CD19 in two patients (patients #01 and 02) approximated the expression level seen in $CD19^+$ B cells, with a unimodal pattern (**Figure 3B**). In the remaining four $CD19^+$ patients, we observed a continuum of CD19 expression levels on AML cells, ranging from the level seen in $CD19^+$ B cells to that of T cells (range: 0 to 4 log; **Figure 3B**). Importantly, internal staining of the leukemic fusion protein RUNX1::ETO demonstrated a strong correlation with CD19 positivity (patient #01 and one additional primary BMMC sample: #08; **Figure 3C** and **S3A**). Given the success of blinatumomab in the treatment of BCP-ALL, we also investigated how the CD19 expression level on $CD19^+$ t(8;21) AML samples (RL048 PDX and patient #08) compared to that on two primary BCP-ALL BMMC samples. While the CD19 MFI in AML patient #08 was lower compared to both BCP-ALL samples, the MFI of the AML PDX sample was just as high (ALL patient #02) or even higher compared to the BCP-ALL samples (patient #01) (**Figure 3D**).

Since individual AML cells in the BM may vary in terms of maturation stages, targeting both immature and more mature AML cells is necessary for sustained therapeutic benefit.[38]

Therefore, we next sought to investigate the CD19 expression on different AML subpopulations, including $CD34^+CD38^-$ cells that encompass the leukemic stem cell (LSC) compartment, as well as those with a $CD34^+CD38^+$ phenotype. Performing flow cytometry on three samples (AML patients #01, #08, and RL048 PDX cells), we observed that nearly all $CD34^+CD38^-$ immature progenitors were positive for CD19 (**Figure 3E** and **S3BC**). These data are in line with previous data in two adults with t(8;21) AML showing that 77 and 91% of $CD34^+CD38^-$ cells were $CD19^+$, respectively.[39, 40] Furthermore, using a more extended flow cytometry panel for analysis of BMMCs from patient #01, we identified CD19 to be expressed on LSCs ($CD34^+CD38^-CD45RA^+$) but not on normal stem cells ($CD34^+CD38^-CD45RA^-$; **Figure 3D**). Similar to immature subpopulations, virtually all $CD34^+CD38^+$ blasts were positive for CD19. Moreover, we noted CD19 expression on both $CD34^+CD38^+CD11b^+$ and $CD34^+CD38^+CD11b^-$ cells, indicating CD19 expression on both more and less mature AML cells (**Figure 3D** and **S3B, S3C**). Taken together, these observations highlight that, in case of high overall AML CD19 expression, both primitive and more differentiated AML cells are potential targets of CD19-directed immunotherapies in $CD19^+$ t(8;21) AML, encouraging exploration of their *ex vivo* killing efficiency.

Blinatumomab is capable of activating T cells when bound to AML cells

Given the possibility of defective immune synapse formation between AML- and T cells, impairing proper T cell activation,[41] we next investigated whether blinatumomab-mediated AML-T cell contact could facilitate the activation of T cells. Using genetically engineered Jurkat cells ($CD3^+CD4^+$) that express luciferase upon induction of the IL2 promoter following CD3 activation **(Figure 4A)**, we observed a dose-dependent increase in the luminescent signal in a co-culture of $CD19^+$ AML PDX- and Jurkat cells **(Figure 4B)**, suggesting that blinatumomab can activate CD3 signaling in T cells by binding to $CD19^+$ AML cells. To further validate this finding, we co-cultured healthy donor T cells with $CD19^+$ AML PDX (RL048) cells in the presence or absence of

blinatumomab for 48 hours. Addition of blinatumomab to the RL048 and T cell co-culture led to significant upregulation of the T cell activation markers CD25 (50% marker positivity) and CD137 (90% marker positivity), indicative of potent T cell activation (**Figure 4C**). In summary, these findings demonstrate that blinatumomab can activate T cells when bound to $CD19^+$ AML cells. Based on the T cell activation assay, we identified 1 nM as the optimal concentration of blinatumomab to activate T cells in our co-cultures. Therefore, this concentration was used in subsequent *ex vivo* co-cultures involving blinatumomab.

$CD19^+$ AML is sensitive to immunotherapy-mediated T cell cytotoxicity *ex vivo*

To determine whether AML cells were sensitive to blinatumomab-mediated T cell cytotoxicity, we co-cultured $CD19^+$ AML PDX cells with or without healthy donor T cells for 48 hours, in the absence or presence of blinatumomab. Treatment of PDX cells with 1 nM of blinatumomab induced 40% AML cell killing at a low E:T ratio of 1:10 and almost 90% killing at an E:T ratio of 1:1 (**Figure 4D**). Importantly, absence of allogeneic T cells or blinatumomab led to no or negligible background killing (**Figure 4D**). We next compared the blinatumomab-mediated T cell killing efficiency between AML and BCP-ALL cells, at increasing E:T ratios of healthy donor T cells. Intriguingly, although we observed substantial variation in the killing efficiency among the three BCP-ALL samples, the observed AML cell killing was comparable to that in BCP-ALL in each E:T ratio ($P > 0.05$; **Figure 4E**).

In addition to blinatumomab, CD19-directed CAR T cells have been approved for the treatment of both pediatric and adult BCP-ALL.[13, 15] Therefore, we assessed whether $CD19^+$ t(8;21) AML cells were sensitive to CAR T cell-mediated cytotoxicity. Similar to blinatumomab, co-culture of CAR T cells with primary AML cells at a low E:T ratio of 1:10, led to 40% killing of AML cells within 48 hours, while AML cells were nearly completely eradicated at an E:T ratio of 1:1

(**Figure 4F**). Notably, AML cell viability remained constant in co-cultures with untransduced T cells from the same donor, indicating negligible background killing (**Figure 4F**). Taken together, these findings demonstrate that CD19-directed immunotherapies induce efficient killing of $CD19^+$ AML cells *ex vivo*. These promising data prompted us to investigate whether the BM microenvironment of $CD19^+$ t(8;21) AML patients is supportive of CD19-directed anti-tumor immunity.

The composition of the bone marrow immune microenvironment of t(8;21) AML is comparable with non-leukemic controls but distinct from BCP-ALL

Previous work in AML, BCP-ALL, and various other cancers has shown that the efficacy of bispecific T cell-engagers and adoptive cell therapy largely depends on the presence and function of various immune cell populations in the tumor microenvironment.[8, 42-48] To understand whether pediatric $CD19^+$ t(8;21) AML patients may represent a subgroup with potential to respond to CD19-directed immunotherapies, we characterized their tumor immune microenvironment using immunogenomic computational approaches applied to diagnostic BM bulk RNA-seq data (**Figure 5A**). Towards this end, we deconvoluted the immune cell abundance in the BM of treatment-naïve $CD19^+$ t(8;21) AML (n=5), $CD19^-$ t(8;21) AML (n=5), other AML genotypes (n=30), and non-leukemic controls (n=4) using CIBERSORTx and the TIDE algorithm.[27, 30] In an exploratory analysis, we did not detect differences in the estimated abundance of lymphoid subsets between $CD19^+$- and $CD19^-$ t(8;21) AML (**Figure S4A-G**). Likewise, no difference was observed among myeloid and stromal cell types (**Figure S4H-J**). Therefore, we considered these cases in aggregate for subsequent comparisons (referred to as t(8;21) group; n=10). We did not detect any differences in the abundance of microenvironmental subsets between both AML groups and non-leukemic controls (**Figure 5B-E, S4K-P**). In line with this, multiple RNA-based metrics related to immune function and -escape were similar among the three groups (**Figure 5F-I**). Indeed, T-

and NK cell-related cytolytic activity (comprised of *GZMA*, *GZMH*, *GZMM, GNLY*, *PRF1*) (**Figure 5F**),[31] a 172-gene immune effector dysfunction score (IED172) reflecting T- and NK cell exhaustion and senescence (**Figure 5H**),[32] and HLA I and -II expression in AML patients did not differ from non-leukemic controls (**Figure 5H-I**).[31] These data indicate that the BM immune microenvironment of t(8;21) AML at diagnosis does not harbor a particularly dysfunctional immune effector fraction nor is it highly immunosuppressive in comparison to non-leukemic controls, suggestive of low immune pressure in this AML subtype.

As CD19-directed immunotherapies have led to impressive and durable responses in pediatric BCP-ALL, we next applied our immunogenomic approach to investigate how the diagnostic BM immune microenvironment of pediatric t(8;21) AML (n=10) compared to that of pediatric BCP-ALL (n=209; **Figure 5A**). As anticipated because of the B cell origin of BCP-ALL, we detected a significant enrichment in naïve B cells in comparison to t(8;21) AML (**Figure S4K**). Furthermore, BCP-ALL cases had a significantly higher abundance of MDSCs and were enriched for T- and NK cell exhaustion and senescence, potentially reflecting a prior T- and NK cell response rendered dysfunctional (**Figure 5B** and **G**). On the other hand, CAFs, memory B cells, and plasma cells were significantly increased in t(8;21) AML compared to BCP-ALL, albeit absolute differences were minimal for the latter two (**Figure 5C** and **S4L-M**). Whereas no differences in HLA I expression were detected, HLA II expression was significantly increased in BCP-ALL compared to t(8;21) AML (**Figure 5H-I**), which is likely related to the antigen presenting cell-origin of BCP-ALL cells.[31] Altogether, our immunogenomic approach revealed that the BM microenvironment in pediatric t(8;21) AML is comparable to that of non-leukemic controls but, at least in part, distinct from that of pediatric BCP-ALL.

Autologous T cells from t(8;21) AML patients are functional and induce cytotoxicity upon activation by blinatumomab

Following the characterization of the BM immune microenvironment in t(8;21) AML patients, we sought to evaluate the efficacy of blinatumomab-mediated killing of $CD19^+$ t(8;21) AML cells by autologous T cells present within BMMC samples (n=2), and to compare this to primary BCP-ALL (n=3). Such an autologous killing assay would reveal the functionality of AML T cells compared to those present in BCP-ALL, at the naturally occurring E:T ratio and in the presence of other BMMCs, approximating the *in vivo* composition. The two AML samples contained 4% and 8% $CD3^+$ T cells, respectively, while all three BCP-ALL samples harbored nearly 3% $CD3^+$ T cells. Interestingly, addition of blinatumomab (1 nM) to 1 x 10^5 BMMCs led, in 48 hours, to a reduction in AML cell viability of approximately 50% compared to the viability in the absence of blinatumomab, which was comparable to that seen in the BCP-ALL samples ($P > 0.05$; **Figure 6A**). To confirm that the reduced AML cell numbers were due to blinatumomab-mediated T cell killing, we measured IFN-γ secretion and the expression of activation markers on the autologous T cells. In both AML samples, we found that blinatumomab induced a significant increase in IFN-γ secretion, with the extent proportional to the abundance of T cells in the BM (**Figure 6B**). In addition, the expression of the T cell activation markers CD25 and CD137 on BM T cells increased substantially in response to blinatumomab (**Figure 6C**). For patient #01, matched PB was also available, which allowed for a co-culture of PB-derived T cells and autologous BMMCs for 48 hours with or without blinatumomab. Consistent with the findings with autologous BM T cells, autologous PB T cells, co-cultured with matched BMMCs, showed substantial activation upon treatment with blinatumomab (**Figure 6D**). Accordingly, PB-derived T cells demonstrated effective AML cell killing (**Figure 6E**). Furthermore, this was accompanied by substantial IFN-γ secretion (**Figure 6F**) and increased T cell numbers after treatment (**Figure 6G**). Overall, these findings

demonstrate that autologous T cells from AML patients are capable to induce cytotoxicity upon binding to T cell-engagers, encouraging the exploitation of CD19 as an immunotherapy target in pediatric $CD19^+$ t(8;21) AML.

Discussion

Repurposing immunotherapies that have been approved for other hematological malignancies may not only accelerate the realization of potential clinical benefits, it can also reduce the inherent risks and delays associated with introducing novel agents. The success of CD19-directed immunotherapies in BCP-ALL, as well as in two adults with relapsed $CD19^+$ t(8;21) AML,[17, 18] prompted us to investigate whether CD19 could be a valuable immunotherapy target in pediatric AML. Our study reveals that a subset of pediatric AML patients, in particular those with t(8;21) AML, express CD19 at diagnosis, consistent with findings in adult AML.[33] Importantly, the extent of CD19 expression on AML cells among those classified as having $CD19^+$ AML was heterogeneous, indicating that not all $CD19^+$ t(8;21) AML patients may be suitable candidates for CD19-directed immunotherapy. In those with unimodal and high CD19 expression, CD19 was expressed on nearly all $CD34^+CD38^-$ and $CD34^+CD38^+$ subpopulations, suggesting potential elimination of these AML subpopulations through CD19-directed immunotherapies. Our *ex vivo* studies revealed that blinatumomab was able to induce AML cell killing with an efficacy comparable to that seen in BCP-ALL. Moreover, CAR T cells could effectively eliminate $CD19^+$ AML cells *ex vivo*. Lastly, T- and NK cells in the bone marrow of pediatric t(8;21) AML appeared to be less exhausted and senescent in comparison to pediatric BCP-ALL. Collectively, our study demonstrates the potential of CD19-directed immunotherapies for the treatment of pediatric $CD19^+$ AML.

While pediatric t(8;21) AML has a favorable prognosis following current chemotherapy regimens (5-year OS rate of nearly 90%),[49] alternative therapies are needed to reduce treatment-

related toxicity in newly diagnosed patients, and to improve outcomes in relapsed and refractory disease. The comparable *ex vivo* blinatumomab-mediated killing efficiency in $CD19^+$ t(8;21) AML and BCP-ALL suggests that the successes observed with CD19-directed immunotherapies for BCP-ALL may be seen in $CD19^+$ t(8;21) AML as well. Given that immunotherapies work best at a favorable E:T ratio, a potential setting for the use of CD19-directed immunotherapies could be that of minimal residual disease (MRD)-positivity before allo-SCT or other cellular therapies with curative intent.[50] Furthermore, we envision that these therapies could serve as an alternative to intensive chemotherapy in case of excess toxicity, or as a life-prolonging treatment when curative options are no longer viable. Of relevance, given the heterogeneous expression of CD19 in those classified as having $CD19^+$ AML, flow cytometry should be used to assess the fraction and intensity of AML cells positive for CD19. Moreover, data from our study and others show that a subset of patients with $CD19^-$ AML at diagnosis gained CD19-expression at relapse, highlighting another subgroup that could potentially benefit from CD19-directed immunotherapies as well.[51]

In addition to our *ex vivo* studies, our characterization of the BM immune microenvironment provides insight into the *in vivo* setting, which may further contribute to identifying patients that are likely to benefit from these immunotherapies. Interestingly, our immunogenomic analyses revealed that the BM immune microenvironment in pediatric t(8;21) AML was highly similar to that of non-leukemic controls, suggestive of low immune pressure. In addition, pediatric t(8;21) AML appeared to have a less exhausted and senescent T- and NK cell compartment in comparison to pediatric BCP-ALL. As T- and NK cell exhaustion and senescence have recently been linked to resistance to bispecific antibodies and immune checkpoint inhibitors, the more inert T- and NK cell state in t(8;21) AML could be a favorable starting point for response to CD19-directed immunotherapies.[32]

A limitation of our study is the relatively small number of $CD19^+$ AML samples available for our *ex vivo* studies. Nonetheless, the observed efficacy of CD19-directed immunotherapies was highly similar among the investigated samples, indicating robustness of our findings.

In conclusion, the high frequency of CD19 expression in pediatric t(8;21) AML, in combination with our *ex vivo*- and immunogenomic studies, suggests that CD19 can be exploited as an immunotherapy target in t(8;21) pediatric AML, and potentially in other AML subtypes exhibiting CD19 positivity as well. The eagerly anticipated results of three clinical trials that are investigating CD19-directed immunotherapies in R/R adult (NCT04257175 and NCT03896854) and pediatric AML (NCT02790515) will shed further light on the potential of these therapies in AML. In addition, we have initiated an international registry for pediatric AML patients treated with CD19-directed immunotherapies, which will simultaneously generate relevant knowledge regarding the efficacy and safety of these therapies in the pediatric population.

Acknowledgements

We would like to express our gratitude to all patients and their parents/caregivers for their participation in the research. We are grateful to Anja de Jong (Princess Máxima Center) for acquiring flow cytometry data; Zinia Kwidama for providing AML samples (UMC Amsterdam, location VUmc, The Netherlands), and Tom Reuvekamp and Marisa Westers for fruitful discussions of the data. Feeders for rapid T-cell expansion were kindly provided by dr. Zsolt Sebestyen (UMC Utrecht, The Netherlands). Figures were created with BioRender.com.

Author contributions

F.B., N.W., G.K., and O.H. formulated the study concept and designed experiments. The experiments were performed by F.B., J.B.K., N.W., T.M., M.A., and E.D. CAR T cell generation was performed by N.D., and A.M.C. The AML medium was optimized by A.K.H. Data interpretation was performed by F.B., N.W., and J.B.K. Co-supervising the panel design for identification of leukemic cells in killing assays of primary AML samples was done by J.C. CAR T cell production was supervised by S.N. and J.K. The manuscript was written by F.B, J.B.K., N.W., and O.H. together with T.M. The study was supervised by K.K., C.Z., G.K., and O.H. All authors read and approved the final version of the manuscript.

Data availability

Sequencing data can be accessed from the Gene Expression Omnibus (GSEXXX; normalized counts [GSE IDs will be available upon publication]. Raw sequencing data requests should be addressed to and will be fulfilled by the corresponding author.

References

1. Zwaan CM, Kolb EA, Reinhardt D, et al. Collaborative efforts driving progress in pediatric acute myeloid leukemia. Journal of clinical oncology 2015;33:2949.
2. Hoffman AE, Schoonmade LJ, Kaspers GJ. Pediatric relapsed acute myeloid leukemia: a systematic review. Expert Review of Anticancer Therapy 2021;21:45-52.
3. Rubnitz JE, Kaspers GJ. How I treat pediatric acute myeloid leukemia. Blood 2021;138:1009-1018.
4. Lynch TJ, Bondarenko I, Luft A, et al. Ipilimumab in combination with paclitaxel and carboplatin as first-line treatment in stage IIIB/IV non–small-cell lung cancer: results from a randomized, double-blind, multicenter phase II study. Journal of clinical oncology 2012;30:2046-2054.
5. Kantarjian H, Stein A, Gökbuget N, et al. Blinatumomab versus chemotherapy for advanced acute lymphoblastic leukemia. New England Journal of Medicine 2017;376:836-847.
6. von Stackelberg A, Locatelli F, Zugmaier G, et al. Phase I/phase II study of blinatumomab in pediatric patients with relapsed/refractory acute lymphoblastic leukemia. Journal of Clinical Oncology 2016;34:4381-4389.
7. Daver N, Alotaibi AS, Bücklein V, et al. T-cell-based immunotherapy of acute myeloid leukemia: Current concepts and future developments. Leukemia 2021;35:1843-1863.
8. Vadakekolathu J, Rutella S. Escape from T-cell targeting immunotherapies in acute myeloid leukemia. Blood 2023.
9. Wijnen NE, Koedijk JB, Klein K, et al. Treating CD33-Positive de novo Acute Myeloid Leukemia in Pediatric Patients: Focus on the Clinical Value of Gemtuzumab Ozogamicin. OncoTargets and Therapy 2023:297-308.
10. Koedijk JB, van der Werf I, Calkoen FG, et al. Paving the way for immunotherapy in pediatric acute myeloid leukemia: Current knowledge and the way forward. Cancers 2021;13:4364.
11. Queudeville M, Ebinger M. Blinatumomab in Pediatric Acute Lymphoblastic Leukemia—From Salvage to First Line Therapy (A Systematic Review). Journal of Clinical Medicine 2021;10:2544.
12. Cappell KM, Kochenderfer JN. Long-term outcomes following CAR T cell therapy: What we know so far. Nature Reviews Clinical Oncology 2023:1-13.
13. Maude SL, Laetsch TW, Buechner J, et al. Tisagenlecleucel in children and young adults with B-cell lymphoblastic leukemia. New England Journal of Medicine 2018;378:439-448.
14. Park JH, Rivière I, Gonen M, et al. Long-term follow-up of CD19 CAR therapy in acute lymphoblastic leukemia. New England Journal of Medicine 2018;378:449-459.
15. Davila ML, Riviere I, Wang X, et al. Efficacy and toxicity management of 19-28z CAR T cell therapy in B cell acute lymphoblastic leukemia. Science translational medicine 2014;6:224ra25-224ra25.
16. Creutzig U, van Den Heuvel-Eibrink MM, Gibson B, et al. Diagnosis and management of acute myeloid leukemia in children and adolescents: recommendations from an international expert panel. Blood, The Journal of the American Society of Hematology 2012;120:3187-3205.
17. Plesa A, Labussière-Wallet H, Hayette S, et al. Efficiency of blinatumomab in at (8; 21) acute myeloid leukemia expressing CD19. Haematologica 2019;104:e487-e488.
18. Danylesko I, Jacoby E, Yerushalmi R, et al. Remission of acute myeloid leukemia with t (8; 21) following CD19 CAR T-cells. Leukemia 2020;34:1939-1942.
19. Dutch Foundation for Quality Assessment in Medical Laboratories

Volume 2023.

20. Kellaway SG, Potluri S, Keane P, et al. Leukemic stem cells activate lineage inappropriate signalling pathways to promote their growth. Nat Commun 2024;15:1359.
21. Marcu-Malina V, Heijhuurs S, van Buuren M, et al. Redirecting αβ T cells against cancer cells by transfer of a broadly tumor-reactive γδT-cell receptor. Blood 2011;118:50-9.
22. van Belzen IA, Cai C, van Tuil M, et al. Systematic discovery of gene fusions in pediatric cancer by integrating RNA-seq and WGS. BMC cancer 2023;23:618.
23. Hehir-Kwa JY, Koudijs MJ, Verwiel ET, et al. Improved gene fusion detection in childhood cancer diagnostics using RNA sequencing. JCO precision oncology 2022;6:e2000504.
24. Graves-Lindsay T, Albracht D, Fulton RS, et al. Evaluation of GRCh38 and de novo haploid genome assemblies demonstrates the enduring quality of the reference assembly. 2017.
25. Frankish A, Carbonell-Sala S, Diekhans M, et al. GENCODE: reference annotation for the human and mouse genomes in 2023. Nucleic acids research 2023;51:D942-D949.
26. Koedijk JB, van Beek TB, Vermeulen MA, et al. Case Report: Immune dysregulation associated with long-lasting regression of a (pre) leukemic clone. Frontiers in Immunology 2023;14.
27. Newman AM, Steen CB, Liu CL, et al. Determining cell type abundance and expression from bulk tissues with digital cytometry. Nature biotechnology 2019;37:773-782.
28. Wang Y, Cai Y-y, Herold T, et al. An immune risk score predicts survival of patients with acute myeloid leukemia receiving chemotherapy. Clinical Cancer Research 2021;27:255-266.
29. Penter L, Liu Y, Wolff JO, et al. Mechanisms of response and resistance to combined decitabine and ipilimumab for advanced myeloid disease. Blood, The Journal of the American Society of Hematology 2023;141:1817-1830.
30. Jiang P, Gu S, Pan D, et al. Signatures of T cell dysfunction and exclusion predict cancer immunotherapy response. Nature medicine 2018;24:1550-1558.
31. Dufva O, Pölönen P, Brück O, et al. Immunogenomic landscape of hematological malignancies. Cancer Cell 2020;38:380-399. e13.
32. Rutella S, Vadakekolathu J, Mazziotta F, et al. Immune dysfunction signatures predict outcomes and define checkpoint blockade–unresponsive microenvironments in acute myeloid leukemia. The Journal of Clinical Investigation 2022;132.
33. Kita K, Nakase K, Miwa H, et al. Phenotypical characteristics of acute myelocytic leukemia associated with the t (8; 21)(q22; q22) chromosomal abnormality: frequent expression of immature B-cell antigen CD19 together with stem cell antigen CD34. Blood 1992.
34. Tiacci E, Pileri S, Orleth A, et al. PAX5 expression in acute leukemias: higher B-lineage specificity than CD79a and selective association with t (8; 21)-acute myelogenous leukemia. Cancer research 2004;64:7399-7404.
35. Ray D, Kwon SY, Tagoh H, et al. Lineage-inappropriate PAX5 expression in t(8;21) acute myeloid leukemia requires signaling-mediated abrogation of polycomb repression. Blood 2013;122:759-69.
36. Chan LN, Chen Z, Braas D, et al. Metabolic gatekeeper function of B-lymphoid transcription factors. Nature 2017;542:479-483.
37. Dick JE. Stem cell concepts renew cancer research. Blood 2008;112:4793-4807.
38. McKenzie MD, Ghisi M, Oxley EP, et al. Interconversion between Tumorigenic and Differentiated States in Acute Myeloid Leukemia. Cell Stem Cell 2019;25:258-272.e9.
39. Terwijn M, Zeijlemaker W, Kelder A, et al. Leukemic stem cell frequency: a strong biomarker for clinical outcome in acute myeloid leukemia. PloS one 2014;9:e107587.

40. Van Rhenen A, Moshaver B, Kelder A, et al. Aberrant marker expression patterns on the CD34+ CD38− stem cell compartment in acute myeloid leukemia allows to distinguish the malignant from the normal stem cell compartment both at diagnosis and in remission. Leukemia 2007;21:1700-1707.
41. Le Dieu R, Taussig DC, Ramsay AG, et al. Peripheral blood T cells in acute myeloid leukemia (AML) patients at diagnosis have abnormal phenotype and genotype and form defective immune synapses with AML blasts. Blood, The Journal of the American Society of Hematology 2009;114:3909-3916.
42. Zhao Y, Aldoss I, Qu C, et al. Tumor-intrinsic and-extrinsic determinants of response to blinatumomab in adults with B-ALL. Blood, The Journal of the American Society of Hematology 2021;137:471-484.
43. Feucht J, Kayser S, Gorodezki D, et al. T-cell responses against CD19+ pediatric acute lymphoblastic leukemia mediated by bispecific T-cell engager (BiTE) are regulated contrarily by PD-L1 and CD80/CD86 on leukemic blasts. Oncotarget 2016;7:76902.
44. Duell J, Dittrich M, Bedke T, et al. Frequency of regulatory T cells determines the outcome of the T-cell-engaging antibody blinatumomab in patients with B-precursor ALL. Leukemia 2017;31:2181-2190.
45. Uy GL, Aldoss I, Foster MC, et al. Flotetuzumab as salvage immunotherapy for refractory acute myeloid leukemia. Blood, The Journal of the American Society of Hematology 2021;137:751-762.
46. Friedrich MJ, Neri P, Kehl N, et al. The pre-existing T cell landscape determines the response to bispecific T cell engagers in multiple myeloma patients. Cancer Cell 2023;41:711-725. e6.
47. Bagaev A, Kotlov N, Nomie K, et al. Conserved pan-cancer microenvironment subtypes predict response to immunotherapy. Cancer cell 2021;39:845-865. e7.
48. Koedijk JB, van der Werf I, Penter L, et al. A multidimensional analysis reveals distinct immune phenotypes and tertiary lymphoid structure-like aggregates in the bone marrow of pediatric acute myeloid leukemia. medRxiv 2023:2023.03. 03.23286485.
49. Reedijk A, Klein K, Coebergh J, et al. Improved survival for children and young adolescents with acute myeloid leukemia: a Dutch study on incidence, survival and mortality. Leukemia 2019;33:1349-1359.
50. Subklewe M, Bücklein V, Sallman D, et al. Novel immunotherapies in the treatment of AML: is there hope? Hematology 2023;2023:691-701.
51. Lambo S, Trinh DL, Ries RE, et al. A longitudinal single-cell atlas of treatment response in pediatric AML. Cancer Cell 2023;41:2117-2135. e12.

544 **Table 1.** Baseline characteristics of $CD19^+$ pediatric AML patients at diagnosis.

Characteristics		**$CD19^+$ AML**
	N	**n (%) or median (range)**
Age at diagnosis (years)	18	10.5 (1-17)
Sex	18	
Male		14 (78)
Female		4 (22)
Hemoglobin (g/dL)	14	5.1 (3.6-7.3)
WBC ($x10^9$/L)	14	11.2 (0.9-70)
Platelets ($x10^9$/L)	14	47.5 (22-343)
Percentage leukemic cells		
Bone marrow	15	54.0 (9-94)
Peripheral blood	9	55.0 (12-80)

545

546

Figure legends

Figure 1. CD19 expression among pediatric AML patients.

(A) Incidence of CD19 positivity among newly diagnosed and relapsed pediatric AML patients. (B) Cytogenetic alterations observed in $CD19^+$ pediatric AML patients. NA=not available. (C) Incidence of the t(8;21) subtype across the total cohort, and the incidence of CD19 positivity among all t(8;21) patients.

Figure 2. Transcriptomic differences between $CD19^+$ and $CD19^-$ t(8;21) AML.

(A) Heatmap showing the expression of the top up- and downregulated genes between $CD19^+$- (n=6) and $CD19^-$ (n=3) t(8;21) AML for each patient. The color bar indicates the logarithmically scaled and normalized gene expression values. (B) Volcano plot showing the differentially expressed genes between $CD19^+$- (n=6) and $CD19^-$ t(8;21) AML. (C) Gene set enrichment analysis plot showing enriched and depleted phenotypes and pathways in $CD19^+$- compared to $CD19^-$ t(8;21) AML. FDR <0.05 was considered significant. NES: normalized enrichment score. FDR: false discovery rate.

Figure 3. Overall and subpopulation-specific CD19 expression in $CD19^+$ t(8;21) AML.

(A) The gating strategy applied to myeloid blasts to identify CD19 positive populations. (B) Overview of the overall CD19 expression among $CD45^{dim}SSC\text{-}A^{low}CD34^+$ blasts in the bone marrow. Data were retrieved from available diagnostic files of six $CD19^+$ t(8;21) AML patients (patient #01-06) and one $CD19^-$ t(8;21) AML patient (patient #07; reference) and were compared to the CD19 expression on T cells (as $CD19^-$ control) and B cells (as $CD19^+$ control). (C) Co-expression of CD19 and RUNX1::ETO among the myeloid blasts present in the bone marrow from patient #01. (D) Comparison of CD19 expression between AML PDX (RL048), one primary sample (patient #08), and two primary BCP-ALL samples. ΔMFI is calculated by subtracting the MFI of CD19 in stained samples from the corresponding unstained samples. (E) CD19 expression among leukemic stem cells ($CD34^+CD38^-CD45RA^+$) and more mature subpopulations ($CD34^+CD38^+CD11b^+$) phenotypes in patient #01. LSC: leukemic stem cell; PDX: patient-derived xenograft.

Figure 4. T cell activation and/or AML cell cytotoxicity mediated by blinatumomab and CAR T cells.

(A) Illustration of the T cell activation bioassay. (B) The luminescent signal intensity upon addition of blinatumomab to $CD19^+$ AML PDX and Jurkat cells (n=2 technical replicates). (C) Expression of the T cell activation markers upon addition of blinatumomab and/or PDX cells compared to healthy donor T cells alone. (D) Effect of 1 nM blinatumomab on the viability of PDX cells at various effector-to-target (E:T) ratios using healthy donor T cells after 48 hours. Data points represent technical replicates. (E) Comparison of blinatumomab-induced cytotoxicity in AML (n=2: patient #08 and PDX) and BCP-ALL patient samples (n=3), after 48 hours. Data represent mean ±SD. *t*-test was performed between each E:T ratio in AML versus BCP-ALL. (F) The viability of primary AML cells (patient #08) after 48 hours of co-culture with CAR T cells or untransduced T cells (control) at different E:T ratios. Data points represent technical replicates. J: Jurkat cells; P: PDX (patient-derived xenograft) cells; bead: CD3/CD28 Dynabeads; B or blin: Blinatumomab. E: effector (T cells); T: target (AML).

Figure 5. Characterization of the bone marrow immune microenvironment of t(8;21) AML using immunogenomic analyses.

(A) Cohort overview for the characterization of the bone marrow (BM) immune microenvironment in pediatric AML, pediatric BCP-ALL, and non-leukemic controls. The non-leukemic controls are four pediatric patients with early-stage rhabdomyosarcoma without malignant BM infiltration (methods). (B-I) Comparison of the abundance of various cell populations and gene signatures among t(8;21) AML patients, AML patients with other cytogenetic alterations, BCP-ALL patients, and non-leukemic controls. Data are presented as median with quartiles and range. The statistical tests used include the Kruskal-Wallis test with Dunn's post-hoc test for multiple comparisons. In case two *P* values are shown, the upper one indicates the result of the Kruskal-Wallis test, while the lower *P* values indicate the result of Dunn's test. MDSC: myeloid-derived suppressor cell; CAF: cancer-associated fibroblast; NK: natural killer; IED172: 172-gene immune effector dysfunction score; HLA: human leukocyte antigen.

Figure 6. T cells from bone marrow and peripheral blood of t(8;21) patients are functional and actively induce cytotoxicity upon blinatumomab administration

(A) Cytotoxicity of autologous bone marrow (BM)-derived T cells upon addition of 1 nM blinatumomab to BM mononuclear cells (MCs) from AML (n=2) and BCP-ALL (n=3) samples after 48 hours. t-test was performed to compare results for blinatumomab-treated AML and BCP-ALL

samples (B) Relative interferon (IFN)-γ measurement in the supernatant of two BMMC AML samples; positive control: 125 pg/mL recombinant IFN-γ protein, n= 3 technical replicates. (C-D) Changes of the activation markers on $CD3^+$ T cells present in the BMMC sample (patient #08) (C) or derived from peripheral blood (patient #01) (D). (E) Cytotoxicity of autologous peripheral blood-derived $CD3^+$ T cells upon co-culture with matched BMMCs from patient #01 after 48 hours; n=3 technical replicates. (F) Relative IFN-γ measurement in the supernatant of BMMCs from patient #01 upon co-culture with matched BMMC cells at different E:T ratios. The + and ++ in the table beneath show the ratio of T cells to AML cells, respectively. Absorbance values were normalized to the corresponding value with $CD3^+$ T cells alone; positive control: 125 pg/ml recombinant IFN-γ, n= 3 technical replicates. CTRL: control. (G) Changes in the number of peripheral blood-derived $CD3^+$ T cell numbers in the presence or absence of 1 nM blinatumomab and in co-culture with BMMCs from patient #01 after 48 hours. Cell numbers for each condition (varying E:T ratios) were normalized to the corresponding condition without blinatumomab.

Figure 1

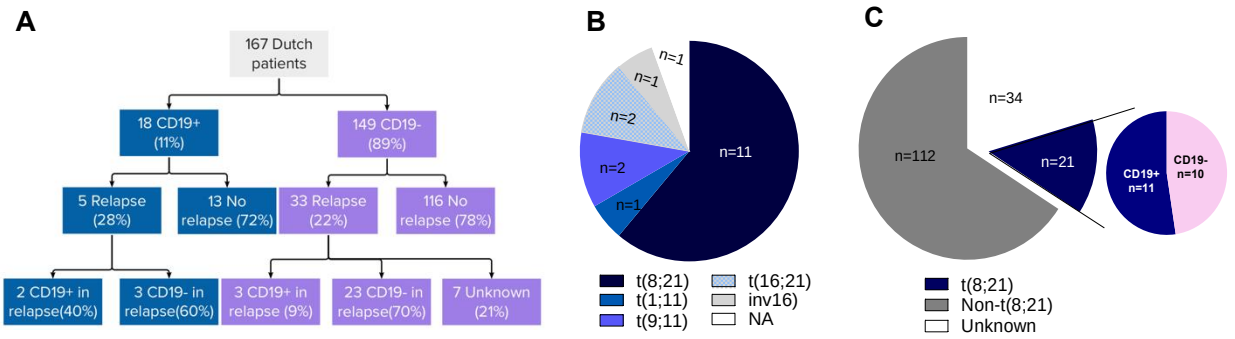

Figure 2

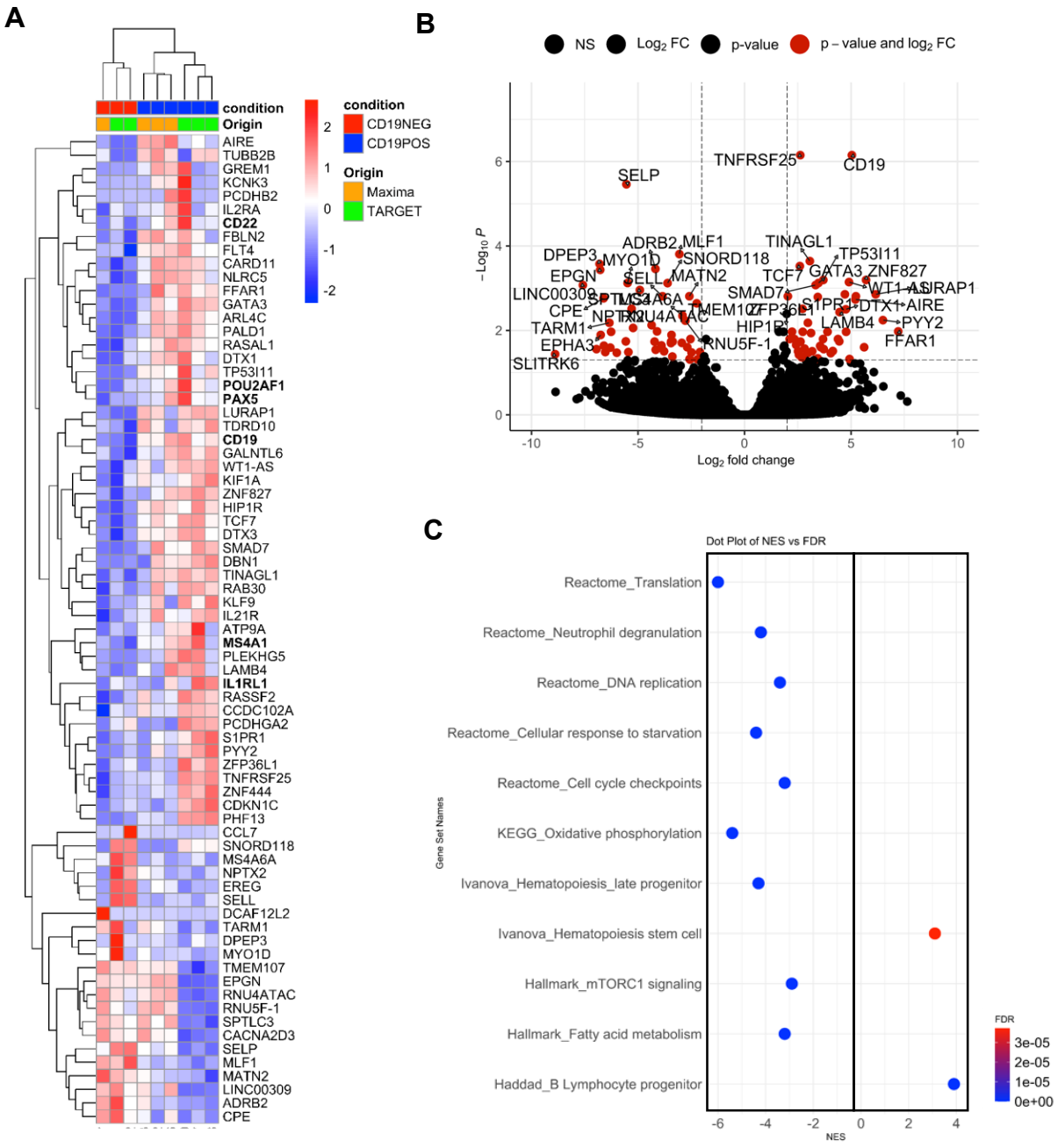

Figure 3

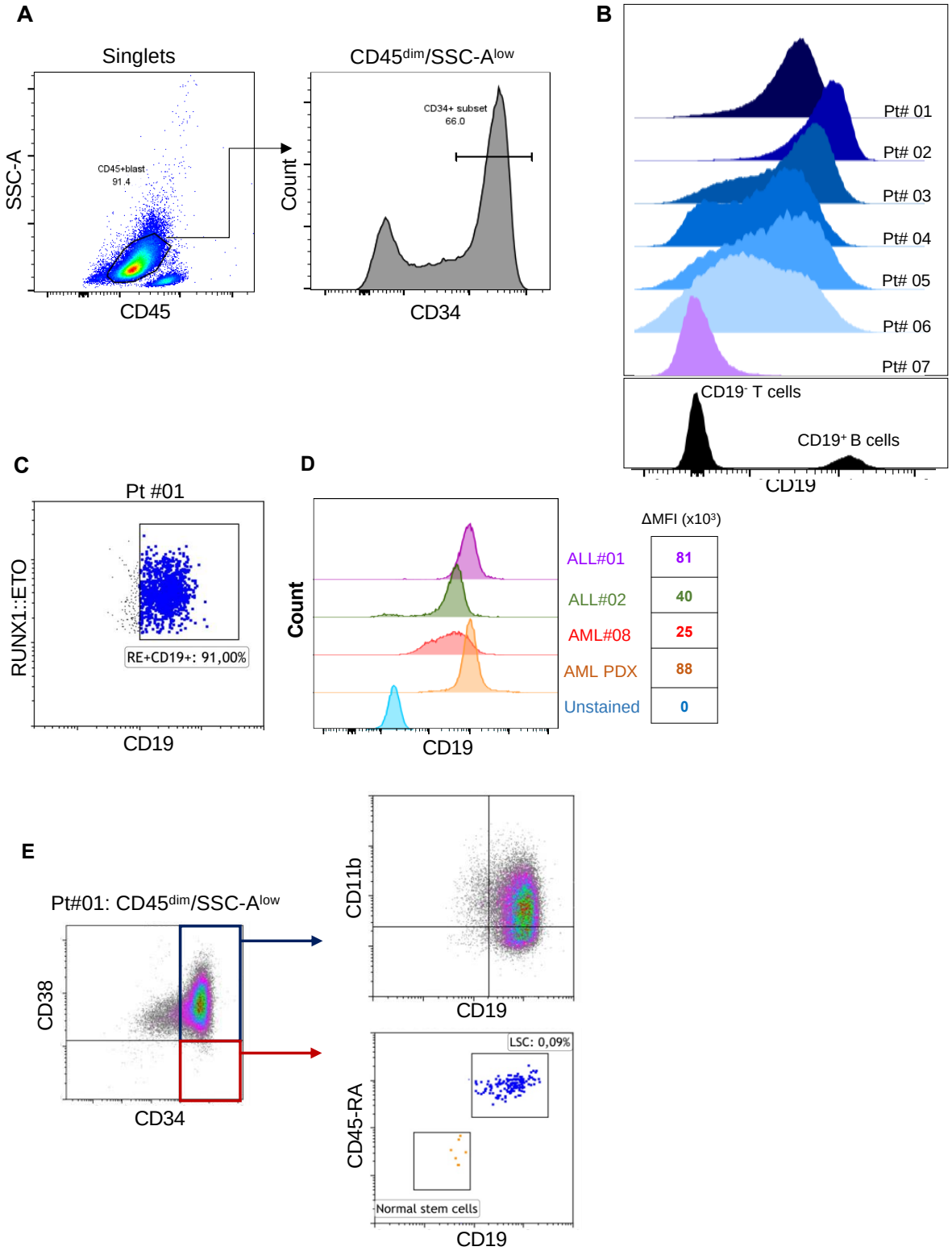

628

Figure 4

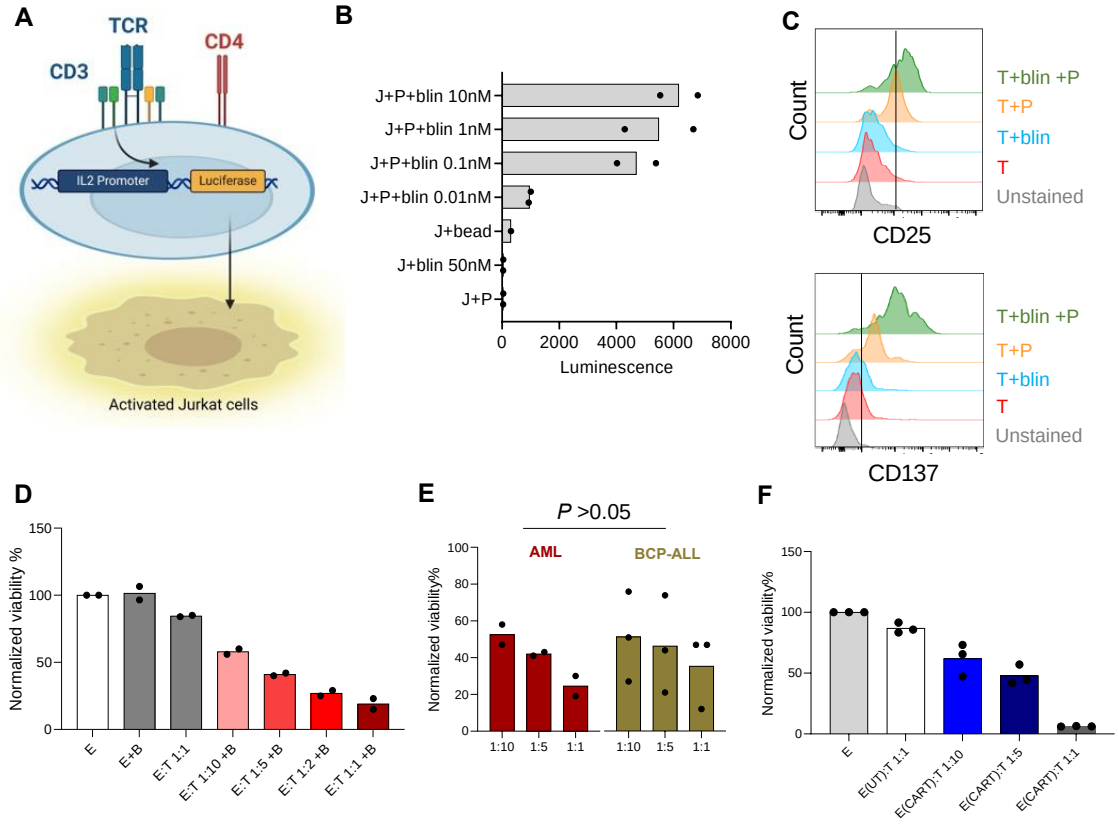

629

Figure 5

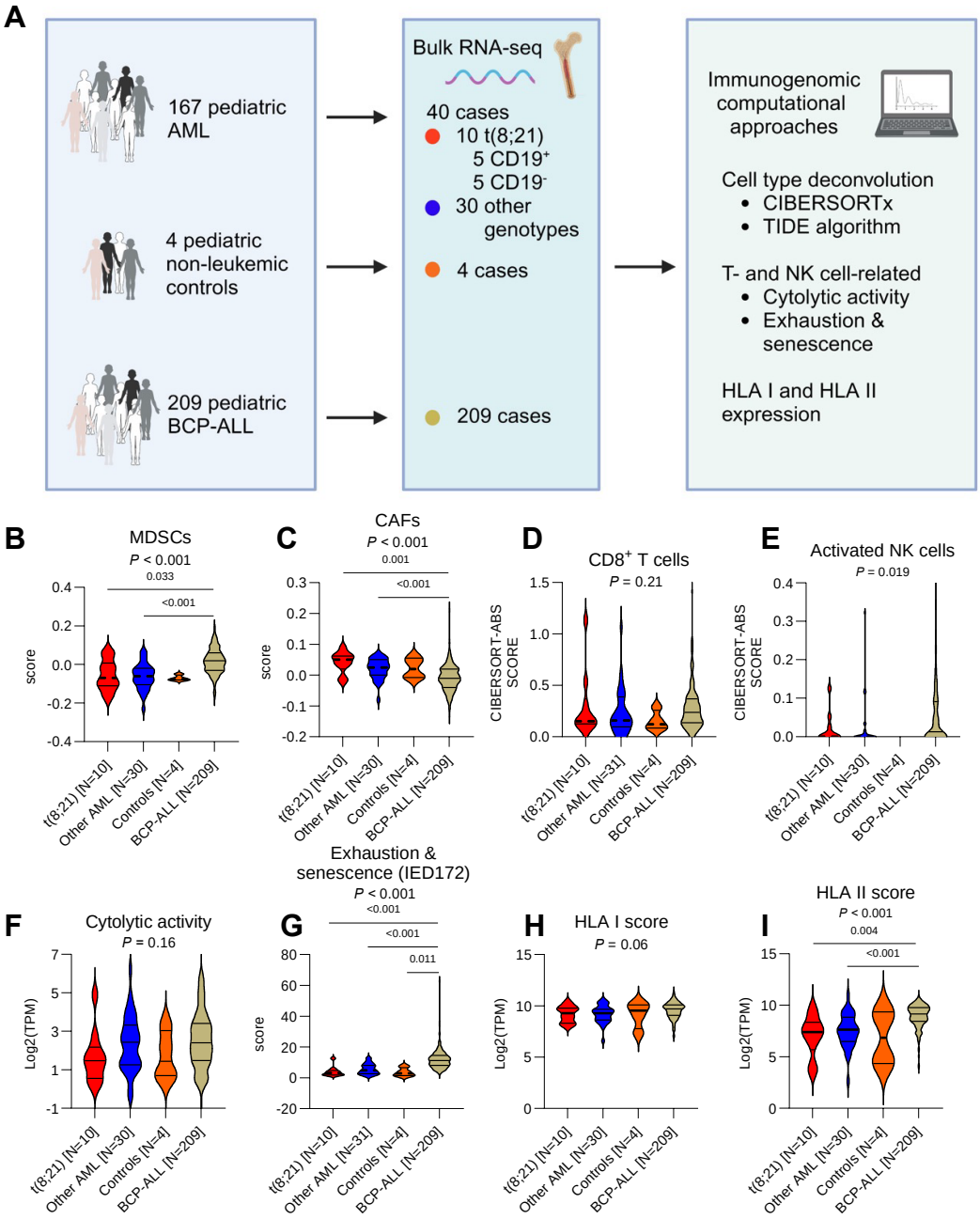

630

631

Figure 6

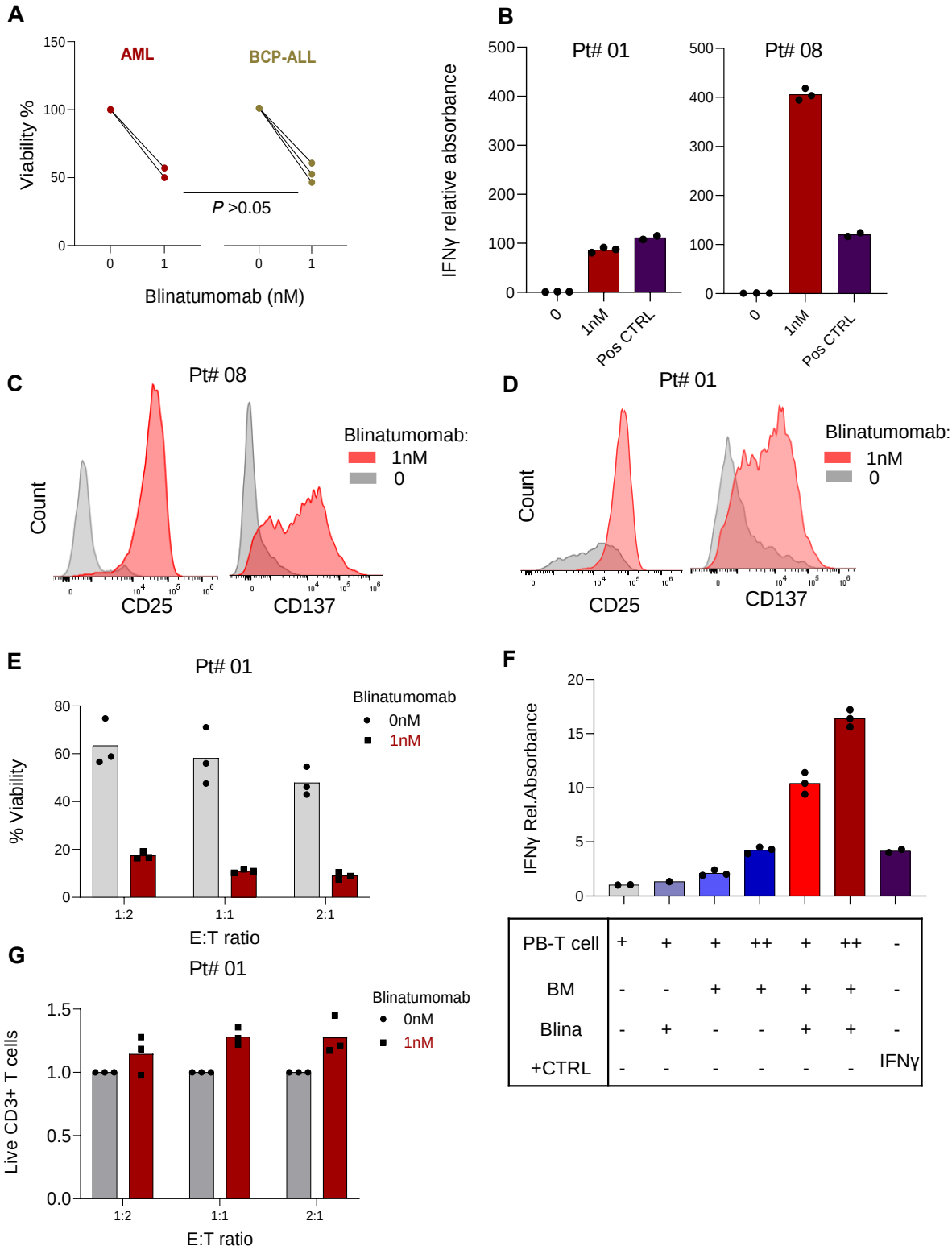

632